Know the single-receptor sensing limit? Think again.

Gerardo Aquino[1], Ned S. Wingreen[2], and Robert G. Endres[1,*]

1 Department of Life Sciences & Centre for Integrative Systems Biology and Bioinformatics, London, United Kingdom 2 Department of Molecular Biology, Princeton University, Princeton, New Jersey 08544, USA

**∗ E-mail: r.endres@imperial.ac.uk**

Abstract

How cells reliably infer information about their environment is a fundamentally important question. While sensing and signaling generally start with cell-surface receptors, the degree of accuracy with which a cell can measure external ligand concentration with even the simplest device - a single receptor - is surprisingly hard to pin down. Recent studies provide conflicting results for the fundamental physical limits. Comparison is made difficult as different studies either suggest different readout mechanisms of the ligand-receptor occupancy, or differ on how ligand diffusion is implemented. Here we critically analyse these studies and present a unifying perspective on the limits of sensing, with wide-ranging biological implications.

Introduction

In 1977, physicists Howard Berg and Edward Purcell published their results on the fundamental biological problem of sensing [1]. The question they addressed was how accurately a biological cell, viewed as a tiny measurement device, can sense its chemical environment using cell-surface receptors. The paper is not only highly cited, but, more importantly, a large fraction of the citations stems from the last ten years, demonstrating how far ahead of its time the study was. In essence, the message of the paper was simple: sensing in the microscopic world boils down to counting molecules, which arrive at the cell surface by diffusion. Humans encounter a similar limit when we try to see in the near dark as our photoreceptors count single photons [2]. Berg and Purcell's paper has influenced many fields of quantitative biology, including nutrient scavenging [3, 5, 7], mating [6], signal transduction [7, 7], gene regulation [8], cell division [9–11], and embryonic development [12]. While there is no disagreement on the importance of knowing the fundamental physical limits of sensing, there has been disagreement on what this limit is, even for a single receptor. The analysis here interprets and unifies these studies to yield a coherent picture of the limits of sensing.

Overview

To introduce the topic and to build intuition, we follow Berg and Purcell [1] and begin with simple models for measuring ligand concentration c_0. The first is the Perfect Monitor [1]. This model assumes a permeable sphere of radius a, capable of counting the number of molecules N inside its volume (Fig. 1a). For concreteness, the sphere might represent a bacterial cell. Since the molecules diffuse independently, finding a molecule in one small volume element is independent of finding another one in a different small volume element, and so the number of molecules N will be Poisson distributed. Since for the Poisson distribution the variance equals the mean, i.e. $\delta N^2 = \bar{N}$ (omitting ensemble-averaging brackets for
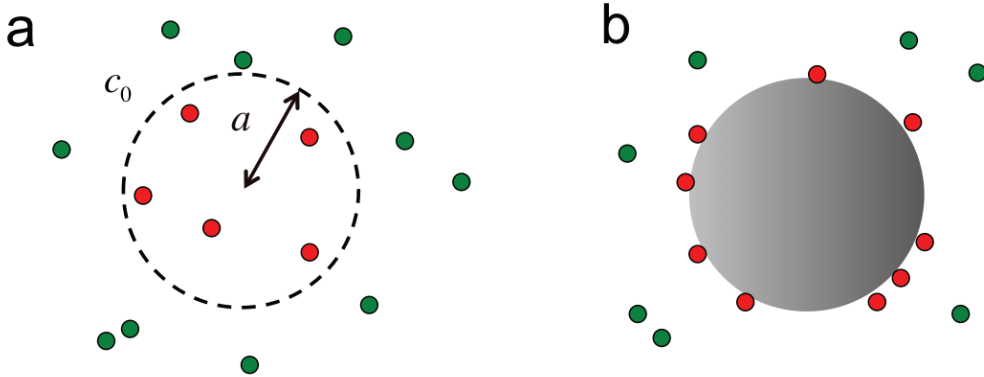
Figure 1. Simple measurement devices for concentration. (a) The Perfect Monitor is permeable to ligand molecules and estimates the concentration c_0 by counting the molecules in its volume during time T. (b) The Perfect Absorber estimates the ligand concentration from the number of molecules incident on its surface during time T.

simplicity of notation), we obtain for a single measurement ("snapshot")

$$\frac{\delta c^2}{c_0^2} = \frac{\delta N^2}{\bar{N}^2} = \frac{1}{\bar{N}} = \frac{1}{c_0 V}, \tag{1}$$

where c_0 is a fixed, given ligand concentration and V is the volume of the monitoring sphere. However, if we assume the Perfect Monitor has some time T available to make a measurement, the uncertainty in the estimate of the true ligand concentration can be further reduced. In time T, the Perfect Monitor can make approximately $M \sim T/\tau_D$ statistically independent measurements, where $\tau_D \sim a^2/D$ is the diffusive turnover time for the molecules inside the sphere. This leads to the reduced uncertainty

$$\frac{\delta c^2}{c_0^2} = \frac{1}{M\bar{N}} = \frac{1}{(T/\tau_D)c_0 V} \sim \frac{1}{Dac_0 T}, \tag{2}$$

where we neglect prefactors for this heuristic derivation. (The exact result is $3/(5\pi Dac_0 T)$, which can be derived by considering autocorrelations of the molecules inside the volume [1].)

However, the Perfect Monitor is not the best one can do. A more accurate estimate can be made if each ligand molecule is only measured *once* rather than being allowed to diffuse in and out of the sphere. Thus, we consider a perfectly absorbing sphere [5], estimating concentration from the number of absorbed ligand molecules N_T in time T, and find (Fig. 1b)

$$\frac{\delta c^2}{c_0^2} = \frac{1}{N_T} = \frac{1}{4\pi Dac_0 T} < \frac{3}{5\pi Dac_0 T} \tag{3}$$

This Perfect Absorber is thus more accurate than the Perfect Monitor (and even more so for spatial gradient sensing by almost a factor of 10) [5]. This result contrasts with Berg and Purcell's original suggestion that rebinding previously measured ligand molecules does not increase the uncertainty in measurement [1]. However, one of their many key insights was that a sphere with many absorbing patches for ligand is nearly as good at sensing as a fully absorbing sphere, making room for multiple receptor types with different ligand specificity without sacrificing much accuracy.
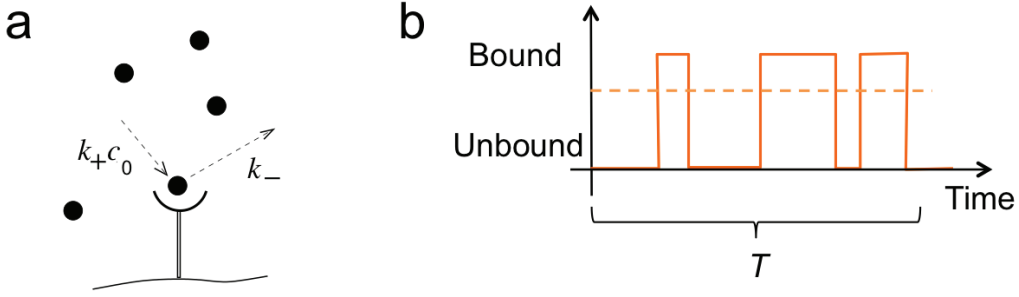
Figure 2. Measuring ligand concentration with a single receptor. (a) A receptor binds ligand with rate k_+c_0 when unbound, and unbinds ligand when bound with rate k_-. (b) Time series of receptor occupancy during time interval T. Berg and Purcell considered the accuracy obtained by taking the average (dashed horizontal line).

Single receptor without ligand rebinding

The single receptor is the simplest measurement device and thus needs to be thoroughly understood. Unfortunately, different approaches to estimating its sensing accuracy have resulted in significant discrepancies. We first disregard the effects of diffusion and rebinding of previously bound ligands, and just consider ligand binding and unbinding.

Consider the receptor shown in Fig. 2a, which binds ligand with rate k_+c_0 when unbound and unbinds ligand with rate k_- when bound. The probability of being bound is then $p = c_0/(c_0 + K_D)$ with $K_D = k_-/k_+$ the ligand dissociation constant. A potential time series of receptor occupancy $\Gamma(t)$ during time T is illustrated in Fig. 2b. Berg and Purcell argued that the best a cell can do to estimate the ligand concentration is to average the occupancy $\Gamma(t)$ over time. For such an average, the variance $\delta\Gamma^2$ was derived from the autocorrelations of occupancy, leading to the relative uncertainty in estimating the ligand concentration

$$\frac{\delta c^2}{c_0^2} = \left(c_0 \frac{\partial p}{\partial c}\right)^{-2} \delta\Gamma^2, \tag{4}$$

where the derivative $\partial p/\partial c$ is the gain or amplification. Naively, one could be tempted to set $\delta\Gamma^2 = p(1-p)$ equal to the variance of a Bernoulli random variable (binomial trials). However, this would correspond to the uncertainty in the concentration estimate following a single instantaneous observation of the state of the receptor, or equivalently to the frequency integral of the noise power spectrum $\delta\Gamma^2 = \int d\omega/(2\pi)S_\Gamma(\omega)$ (see Supplementary Information for details). This snapshot limit can be improved if we assume $T \gg 1/(k_+c_0) + 1/k_-$, i.e. that the receptor is allowed to average over a time T much larger than the correlation time of ligand binding and unbinding. In this case, one can take the low-frequency limit $\delta\Gamma^2 \approx S_\Gamma(\omega = 0)/T$ instead, and Eq. 4 leads to the Berg-Purcell limit for a single receptor

$$\frac{\delta c^2}{c_0^2} = \frac{2\tau_b}{Tp} = \frac{2}{\bar{N}} \rightarrow \frac{1}{2Dac_0(1-p)T}, \tag{5}$$

where $\tau_b = 1/k_-$ is the average duration of a bound interval. The simple formulation as $2/\bar{N}$ follows because the average number of binding and unbinding events in time T is $\bar{N} = T/(\tau_b + \tau_u)$, where $\tau_u = (k_+c_0)^{-1}$ is the average duration of an unbound interval. The final result in Eq. 5 follows from detailed balance for diffusion-limited binding.

But is it true that averaging receptor occupancy is the best way to estimate concentration? More recently a limit lower than Eq. 5 was found by applying maximum-likelihood estimation to a time series

$\Gamma(t)$ of receptor occupancy [13]. Here the probability $P(\Gamma, c)$ of observing a time series Γ is maximised with respect to the concentration c. The resulting best estimate of the concentration comes only from the unbound intervals, since only they depend on the rate of binding and thus on the ligand concentration. To obtain a lower limit on the uncertainty the Cramér-Rao bound [14] can be used, leading to

$$\frac{\delta c^2}{c_0^2} \geq \frac{1}{c_0^2 I(c_0)} \to \frac{1}{N}, \tag{6}$$

where $I(c_0) = -\partial^2 \ln(P)/\partial c^2$ is the Fisher information evaluated at c_0 and averaged over all trajectories with the same N (when employing maximum-likelihood estimation it is easier to work with a fixed number of binding/unbinding events N than a fixed time T). The limit on the right-hand side of Eq. 6 is obtained for long time series for which the inequality becomes an equality. Note, however, that a slightly sharper bound $1/(N-2)$ can be obtained when using a further improved estimator (see Supplementary Information). Eq. 6 shows that the uncertainty in Eq. 5 can be reduced by a factor of two. This is because only unbound intervals carry information about the ligand concentration. In contrast, the bound intervals only increase the uncertainty and hence are discarded by the maximum-likelihood procedure.

What does the maximum-likelihood result imply about tuning receptor parameters to minimise the uncertainty? The minimal uncertainty is obtained for N_{max}, the maximal number of binding events provided by very fast unbinding ($k_- \to \infty$). This ideal limit corresponds to the Perfect Absorber from Eq. 3 as every binding event is counted. (However, the increased accuracy comes at the expense of specificity as any ligand molecule dissociates immediately and hence different ligand types cannot be differentiated.) Maximum-likelihood estimation can also be extended to ramp sensing (temporal gradients) [15] and multiple receptors [16, 17].

Adding a downstream signaling molecule cannot increase the accuracy of sensing, in fact this only adds noise. For example, consider an integrating receptor à la Berg and Purcell, which signals while being ligand bound (Fig. 3a) [20]. In this simple network a downstream signaling molecule with concentration n is phosphorylated by ligand-bound receptors with the phosphorylated concentration given by n_p with lifetime τ (beyond this time the protein converts back to the unphosphorylated form). Now, instead of taking the snapshot limit, i.e. the total variance δn_p^2, we time average to reduce the uncertainty. Specifically, let us assume a long averaging time, that is $T \gg \tau \gg 1/(k_+c_0) + 1/k_-$, allowing us to use again the low-frequency limit of the corresponding power spectrum. We then obtain (see Supplementary Information for details)

$$\frac{\delta c^2}{c_0^2} = \left[\frac{2}{\bar{N}_\tau} + \frac{2}{\bar{n}(1-p)^2}\right]\frac{\tau}{T} \tag{7}$$

$$= \underbrace{\frac{2}{\bar{N}}}_{\text{BP limit}} + \underbrace{\left[\frac{2}{\bar{n}(1-p)^2}\right]}_{\text{Poisson-like}}\underbrace{\frac{\tau}{T}}_{\text{time ave}}. \tag{8}$$

Eq. 8 shows that by integrating receptor output one cannot do better than the Berg-Purcell limit, given by the first term. The second term represents additional Poisson-like noise from number fluctuations of the signaling molecule due to imperfect averaging [21]. For $T \gg \tau$ the Berg-Purcell limit is approached from time averaging this noise. While we focus here on averaging in time of stationary stimuli, non-stationary ligand concentrations may be more accurately sensed via non-uniform time averaging, requiring appropriately designed signaling cascades [22].

There has been some confusion about whether sensing actually costs energy. On the one hand, C. H. Bennett pointed out long ago that sensing does not need to cost if done reversibly (and hence extremely slowly) [23]. On the other hand, cells obviously consume energy, e.g. using ATP to phosphorylate proteins. In other words, what energy cost is actually necessary for performing a measurement? As stressed by the authors in [20] the process of sensing in terms of ligand-receptor binding does not need
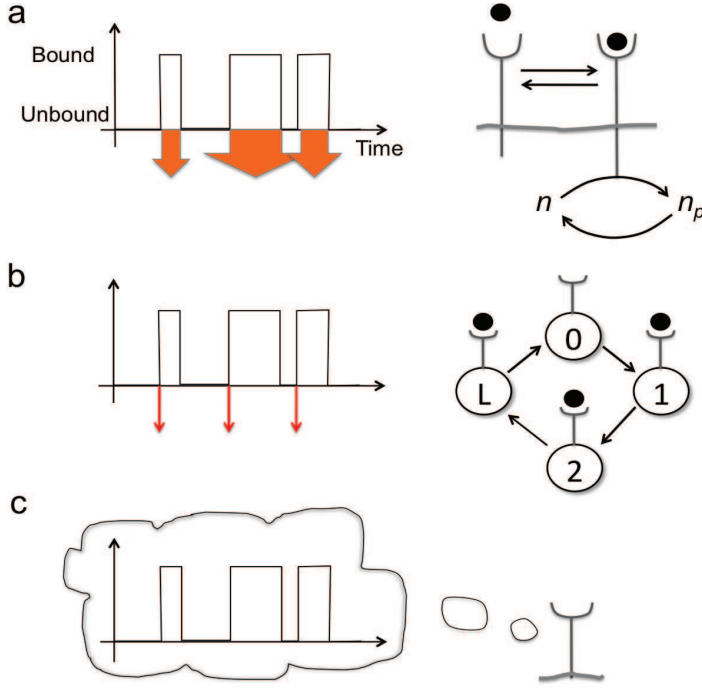
Figure 3. Three schemes of receptor readout. (a) Integrating receptor, which signals while ligand bound (left) [1]. For example, the active receptor might phosphorylate a protein with concentration n. The concentration of the phosphorylated protein is n_p (right). (b) Alternatively, the receptor may signal in generic bursts at onset of ligand binding (left) [13]. This scheme can be implemented by an energy-driven cycle of L active/bound receptor conformations, which reduces variability (right) [18]. (c) A receptor could also retain a memory of previous binding and unbinding events, potentially improving its accuracy of sensing [5].

to cost energy if done using an equilibrium receptor in the spirit of Berg and Purcell. However, to accurately infer the external ligand concentration, the cell needs to time average, which cannot be done without consuming energy. This is in line with the Landauer erasure principle [24], which predicts a lower theoretical limit of energy consumption of a computation. In essence, to keep a record of the past for averaging, old information needs to be erased and time-reversal symmetry broken [25]. Time averaging can be implemented by phosphorylation of a downstream protein: when the receptor is bound it phosphorylates and when unbound it dephosphorylates. Since these are energetically driven reactions the reverse reaction, e.g. dephosphorylation by a bound receptor is extremely unlikely, and time averaging is very efficient. The issue of the cost was avoided in Berg and Purcell's analysis by providing an effective averaging time T without specifying how this averaging is achieved.

How is the maximum-likelihood result, Eq. 6, useful? The maximum-likelihood result makes interesting predictions about sophisticated sensing strategies cells might employ. For example, to implement maximum likelihood in the fast unbinding limit a receptor should only signal upon a ligand-binding event as illustrate in Fig. 3b (thin arrows), rather than continuously signaling while ligand is bound (see [26] for further discussion). How can the cell achieve such short and well-defined signaling durations? Reducing variability and achieving determinism requires energy consumption and irreversible cycles [18]. Examples may include ligand-gated ion channels [27] and single-photon responses in rhodopsin of rod cells [28].

Maximum likelihood provides another valuable insight - it shows that information from an estimate

and memory from a prior are equivalent, and both can contribute to lowering the uncertainty (Fig. 3c). This kind of receptor "learning" from past estimates can be implemented using the Bayesian Cramér-Rao bound for the uncertainty. Using prior information $I(\lambda)$, one obtains [5]

$$\frac{\delta c^2}{c_0^2} = -\frac{1/c_0^2}{\underbrace{I(c_0)}_{\text{Fisher info.}} + \underbrace{I(\lambda)}_{\text{prior}}} = \frac{1}{2N}, \tag{9}$$

assuming the prior had variance $1/N$, identical to the actual measurement. Importantly, memory can even help in fluctuating environments if a filtering scheme is implemented by the cell [5]: if the environment fluctuates weakly and/or with long temporal correlations, memory improves precision significantly. If, on the other hand, the environment fluctuates very strongly and/or without any correlations, the cell can still rely on the current measurement (and disregard memory). A form of memory is implemented by receptor methylation in bacterial chemotaxis [29], and in principle memory could be implemented by any slow process in the cell, e.g. the expression of LacY permease in enzyme induction in the lac system [30], or the remodelling of the actin cortex in eukaryotic chemotaxis [31, 32].

Single receptor with ligand rebinding

So far we have neglected the possibility of rebinding by previously bound ligands. In fact, the role of ligand rebinding in the accuracy of sensing is a tricky issue, because rebinding can introduce non-trivial correlations between binding events. In practice, these correlations can only be included approximately in analytical calculations, and so the question is how to proceed. Originally Berg and Purcell made the reasonable suggestion that a molecule that fails to bind to a receptor may return to the receptor by diffusion and rebind, and that this effect may be included by considering diffusion-limited binding with a renormalised receptor size [1]. However, the question is how to formally separate ligand binding and unbinding from ligand diffusion.

Bialek and Setayeshgar addressed this problem by coupling ligand-receptor binding and unbinding to the diffusion equation [7]. Assuming that the averaging time is long compared to the typical binding and unbinding time, the low-frequency limit can be used. This results in

$$\frac{\delta c^2}{c_0^2} = \frac{2}{k_+ c_0 (1-p)T} + \frac{1}{\pi D a c_0 T} \tag{10}$$

with a now the size of the receptor. Equation 10 indicates noise contributions from two independent sources. According to Ref. [7], the first term represents binding and unbinding noise and depends on the rate parameters, while the second depends on diffusion and was interpreted as a Berg-Purcell-like noise floor. However, we argue for a different interpretation: For diffusion-limited binding, the first term in Eq. 10 is not zero, but rather k_+ needs to be set to a Kramer-like expression, which is proportional to the diffusion constant [33] and an Arrhenius factor at most equal to one [34]. Due to their dependence on the diffusion constant, both terms can be combined [35]. Indeed, for diffusion-limited binding it is the first, not the second term of Eq. 10 that captures the Berg-Purcell limit. Since Berg and Purcell did not consider rebinding by diffusion, the second term constitutes increased noise due to a rebinding correction that does not arise in Berg and Purcell's derivation [1]. Bialek and Setayeshgar also applied their method to multiple receptors, and showed that the second term can introduce correlations among receptors, as ligand unbinding at one receptor can lead to re-binding at another nearby receptor [35, 36]. Hence, while multiple independent receptors allow for spatial averaging [37], mutual rebinding among different receptors by diffusion increases the uncertainty of sensing.

More recently, Kaizu *et al.* readdressed this problem [8] by applying a formalism developed by Agmon and Szabo for diffusion-influenced reactions [39]. By calculating survival probabilities of bimolecular

reactions with a number of simplifying assumptions (see below), they obtained for the relative uncertainty of a single receptor

$$\frac{\delta c^2}{c_0^2} = \frac{2}{k_+ c_0 (1-p)T} + \frac{1}{2\pi D a c_0 (1-p)T}. \tag{11}$$

Similar to Bialek and Setayesghar, there are two noise contributions with the first terms in Eq. 10 and 11 formally identical. The second term is, however, different. While the lost factor 2 in the second term in Eq. 11 can be traced to different definitions of the receptor geometry (cubic in Eq. 10 and spherical in Eq. 11), the factor $1 - p$ in Eq. 11 is missing from Eq. 10. Due to this factor, both terms of the uncertainty in Eq. 11 diverge if the receptor is fully bound on average ($p = 1$), while in Eq. 10 only the first term diverges. Unlike Eq. 10 Kaizu *et al.* made the additional assumption that during a bound interval the external ligand equilibrates. As a result, an unbound ligand molecule cannot diffuse away and rebind at a later time with another ligand bound in between. However, using exact simulations they showed that such delayed rebinding is only a minor effect under biologically relevant conditions. Hence, as the factor $1 - p$ in the second term of Eq. 11 also appears in the Berg-and-Purcell limit, Eq. 5, Kaizu *et al.* argue that their result is more accurate than Eq. 10.

However, we propose a slightly different interpretation of Eq. 11. Similar to [7] we suggest that the second term is not the Berg-Purcell limit (Eq. 5) for diffusion-limited binding since the first term captures the Berg-Purcell limit [8]. As described above, for diffusion-limited binding the first term cannot be neglected. This aside, how may the factor $1 - p$ in the second term be interpreted? In Kaizu *et al.*'s derivation, diffusion means that a ligand molecule enters the ligand pocket of a receptor without actually binding (hence the factor $1 - p$ in the second term since they assume only an unbound receptor can be approached by a ligand molecule). In Bialek and Setayeshgar's derivation, no such factor appears as the second term describes fluctuations in ligand concentration simply in the vicinity of the receptor. Can further insight into the effects of diffusion be obtained by yet an alternative method?

Maximum-likelihood estimation can also be applied to a receptor with ligand diffusion, albeit only in a special case. The probability of observing a time series of receptor occupancy of N binding and unbinding events can be formally written down even with diffusion [13]. However, the rate of binding will depend on the current ligand concentration, which is influenced by the history of all previous binding and unbinding events (even before the first recorded binding event). To estimate the uncertainty, the Cramér-Rao bound can be applied but cannot be evaluated exactly. Nevertheless, for fast diffusion or slow binding an approximate expression can be derived for both 2D and 3D (see Supplementary Information)

$$\frac{\delta c^2}{c_0^2} \approx \frac{1}{N}\left(1 + 2\frac{\Delta c}{c_0}\right) = \frac{1}{k_+ c_0 (1-p_{1/2})T} + \begin{cases} \frac{\ln(4\pi D/(k_+ c_0 a^2))}{2\pi D c_0 (1-p_{1/2})T} & \text{for 2D} \\ \frac{1}{\pi D a c_0 (1-p_{1/2})T} & \text{for 3D} \end{cases}. \tag{12}$$

In Eq. 12 the average local "excess" ligand concentration Δc due to previous binding and unbinding events is $k_+ c_0/(4\pi D) \cdot \ln[4\pi D/(k_+ c_a a^2)]$ in 2D and $k_+ c_0/(2\pi D a)$ in 3D (for the derivation half occupancy $p_{1/2} = 1/2$ is required). The ratios in the excess concentration reflect the competition between rebinding and diffusion. As expected, in 2D this concentration decays more slowly to zero with increasing diffusion constant than in 3D, and also the spatial dependence on the receptor size is weaker in 2D than in 3D.

Coming back to the different receptor models with diffusion, the first term of Eq. 12 produces exactly half the uncertainty of the first terms of Bialek and Setayeshgar (Eq. 10) and Kaizu *et al.* (Eq. 11) by utilizing only the unbound time intervals. However, due to factor $1 - p$ the second term of Eq. 12 resembles the second term of Kaizu *et al.* (both Eq. 11 and Eq. 12 for 3D use a spherical receptor). This suggests that Kaizu *et al.* is the correct result for the accuracy of sensing by time averaging, while Eq. 12 is the more accurate result when using maximum-likelihood estimation.
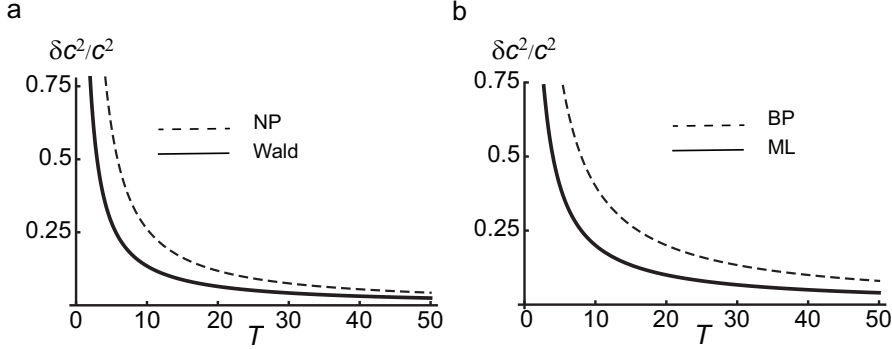
Figure 4. Comparison of decision-making algorithms and fixed-time algorithms. (a) Decision-making algorithms: Wald algorithm (solid curve) has lower uncertainty than fixed-time log-likelihood ratio estimation based on the Neyman-Pearson (NP) lemma (dashed curve). Uncertainty is calculated by converting decision error into variance. (b) Uncertainty estimates based on direct measurement of ligand concentration in a fixed amount of time: Maximum-likelihood (ML) estimation (solid curve) based on the Cramér-Rao bound of Fisher information has only half the uncertainty of the Berg-Purcell (BP) limit (dashed curve) for the standard error of the mean concentration. For further details see Supplementary Information.

Single receptor as a decision maker

All the above approaches considered the accuracy based on a fixed measurement time (or number of binding and unbinding events). However, similar to humans, cells might follow a different strategy and approach a problem from a decision-making perspective [9, 40]: either deciding based on existing information or waiting to accumulate more data.

Recently, Siggia and Vergassola considered decision making in the context of cells, proposing that the above maximum-likelihood estimate can further be improved in this way [9]. The simplest implementation of a decision-making strategy is the so-called Wald algorithm [42]. For a single receptor, the Wald algorithm requires calculating the ratio R of the likelihoods of the time series of binding and unbinding events of a receptor Γ (data), conditioned to either of two hypothesised values of external ligand concentration

$$R = \frac{P(\Gamma|c_1)}{P(\Gamma|c_2)}. \tag{13}$$

The cell then concludes that the ligand concentration is c_1 if $R \geq H_1$, that the ligand concentration is c_2 if $R \leq H_2$, or keeps collecting data if $H_1 < R < H_2$. H_1 and H_2 are thresholds that set the probability of error, i.e. concluding the concentration is c_1 if the true concentration is c_2 and vice versa. This algorithm, by not having a fixed-time constraint, can be shown to be optimal, i.e. the average time to make a decision between the two options is shorter than provided by any other algorithm with the same accuracy (decision-error probability).

How can decision making be compared with maximum-likelihood estimation and the Berg-Purcell limit? Siggia and Vergassola suggested a fixed-time log-likelihood-ratio estimation à la Eq. 13 based on the Neyman-Pearson lemma. Due to the fixed-time constraint the Neyman-Pearson algorithm is in spirit similar to maximum-likelihood estimation. Siggia and Vergassola showed that the Wald algorithm leads to a shorter decision-making time, on average, than the Neyman-Pearson algorithm, and so suggested that the Wald algorithm provides the ultimate limit for sensing.

The result for the Wald algorithm indeed shares properties with the maximum-likelihood estimate and the Berg-Purcell limit. All three reveal a dependence of the measurement (decision) time on the inverse

of the square of the difference of concentration (i.e. Δc^2). Although no decision making is involved in maximum-likelihood estimation or the Berg-Purcell limit, one can still conclude that concentrations c_1 and c_2 can be distinguished if the measurement uncertainty is smaller than the difference $\delta c^2 < (c_2 - c_1)^2$, and that, assuming either c_1 or c_2 as the true value, an incorrect decision occurs if measurement returns a value closer to the wrong concentration. This way a decision error can be converted into a type of measurement uncertainty and vice versa (see Supplementary Information for details).

Fig. 4a shows the thus derived uncertainty in measuring a ligand concentration by the Wald algorithm and the Neyman-Pearson lemma as a function of average measurement time. For comparison the maximum-likelihood estimate and the Berg-Purcell limit are shown in Fig. 4b. However, since the fixed-time likelihood algorithms (Neyman-Pearson lemma and maximum-likelihood estimate) do not agree, it is difficult to directly compare Wald with the Berg-Purcell limit. After all, Wald and Neyman-Pearson algorithms are about hypothesis testing and discrimination, while time averaging (Berg-Purcell) and maximum likelihood are about estimation.

What types of algorithm are cells actually implementing? Consider chemotaxis in the bacterium *Escherichia coli* as a prototypical example of chemical sensing. Downstream signaling, especially slow motor switching, could provide a time scale for Berg-Purcell-type time averaging. In contrast, biological systems with hysteresis, that is two different thresholds for activation and deactivation of the downstream pathway, may implement a type of decision-making algorithm. The classical example is the lactose utilisation system in *E. coli*, which can be stimulated by the non-metabolisable 'gratuitous' inducer TMG [30, 40]. When TMG is high enough enzymes of the lac system become induced. Once induced, however, the TMG level must be reduced below a much lower threshold in order to uninduce the lac system.

Outlook

While the question of the physical limits of sensing has been around for decades, only over the last few years has the importance of this question become clear and its predictions testable by quantitative experiments [43, 44]. While current work is mostly about chemical sensing, the limits of sensing other stimuli, such as substrate stiffness during durotaxis (or temperature, pH, particles, and combinations of them, etc.) may be next. For such measurements, the role of domain size and spatial dimension are interesting questions. Measurements are often done inside a cell, on 2D surfaces, or along 1D DNA molecules, and correlations due to rebinding depend on these parameters [45].

The question of the limits of sensing has also opened up completely new directions, including the role of active, energy-consuming sensing strategies [18, 20, 46, 47], and hence the importance of nonequilibrium-physical processes in cell biology. This then connects to the Landauer limit of information erasure and cellular computation in general [48, 49]. In this area, important questions are linking information theory, statistical inference, and thermodynamics e.g. in order to produce generalized second laws [50]. Additionally, analysis may move away from only considering receptors to considering receptors and their downstream signaling pathways, and questions of optimal resource allocation in such pathways emerge [25].

Other areas of study have started to benefit from this work as well, such as gene regulation. For instance, why do cells often use bursty frequency modulation of gene expression under stress and in development [51]? This may either reflect a need for accurately sensing and monitoring chemical cues, or simply enhance robustness, e.g. similar to when information is transmitted between neurons by action potentials. The questions whether cells sense at the physical limit and if so, how they reach it, and how to design experiments to answer these questions will occupy us for a while.

Acknowledgments

References

1. Berg HC, Purcell EM (1977) Physics of chemoreception. Biophys J 20: 193–219.

2. Rieke F, Baylor DA (1998) Single-photon detection by rod cells of the retine. Rev Mod Phys 70: 1027–1036.

3. Dusenberg DB (1998). Spatial sensing of stimulus gradients can be superior to temporal sensing for free-swimming bacteria.

4. Bialek W, Setayeshgar S (2005) Physical limits to biochemical signaling. Proc Natl Acad Sci USA 102: 10040–10045.

5. Endres RG, Wingreen NS (2008) Accuracy of direct gradient sensing by single cells. Proc Natl Acad Sci USA 105: 15749–15754.

6. Noa R, Naama B (2012) Disentengling signaling gradients generated by equivalent sources. J Biol Phys 38: 267–278.

7. Hu B, Kessler DA, Rappel WJ, Levine H (2011) Effects of input noise on a simple biochemical switch. Phys Rev Lett 107: 148101.

8. Tkacik G, Bialek W (2009) Diffusion, dimensionality, and noise in transcription. Phys Rev E 79: 0519101.

9. Howard M (2012) How to build a robust intracellular concentration gradient. Trends Cell Biol 22: 311.

10. Halatek J, Frey E (2012) Highly canalized MinD transfer and MinE sequestration explain the origin of robust MinCDE-protein dynamics. Cell Rep 1: 741–752.

11. Kerr RA, Levine H, Sejnowski TJ, Rappel WJ (2006) Division accuracy in a stochastic model of Min oscillations in Escherichia coli. Proc Natl Acad Sci USA 103: 347.

12. Gregor T, Tank DW, Wieschaus EF, Bialek W (2007) Probing the limits to positional information. Cell 130: 150–164.

13. Endres RG, Wingreen NS (2009) Maximum likelihood and the single receptor. Phys Rev Lett 103: 158101.

14. Cover TM, Thomas JA (2006) Elements of Information Theory. Wiley (2nd edition).

15. Mora T, Wingreen NS (2010) Limits of sensing temporal concentration changes by single cells. Phys Rev Lett 104: 248101.

16. Mortimer D, Dayan P, Burrage K, Goodhill GJ (2010) Optimizing chemotaxis by measuring unbound-bound transitions. Physica D 239: 477–484.

17. Hu B, Chen W, Kessler DA, Rappel WJ, Levine H (2010) Physical limits on cellular sensing of spatial gradients. Phys Rev Lett 105: 048104.

18. Lang A, Fisher CK, Mora T, Mehta P (2014) Thermodynamics of statistical inference by cells. Phys Rev Lett 113: 148103.

19. Aquino G, Tweedy L, Heinrich D, Endres R (2014) Memory improves precision of cell sensing in fluctuating environments. Sci Rep 4: 5688.

20. Mehta P, Schwab DJ (2012) Energetic cost of cellular computation. Proc Natl Acad Sci USA 109: 17978–17982.

21. Paulsson J (2004) Summing up the noise in gene networks. Nature 427: 415–419.

22. Govern CC, ten Wolde PR (2012) Fundamnetal limits on sensing chemical concentrations with linear biochemical networks. Phys Rev Lett 109: 218103.

23. Bennett CH (1973) Logical reversibility of computation. IBM J Res Dev 17: 525.

24. Landauer R (1961) Irreversibility and heat generation in the computing process. IBM J Res Dev 5: 183.

25. Govern CC, ten Wolde PR (2014) Optimal resource allocation in cellular sensing systems. Proc Natl Acad Sci USA 111: 17486-17491.

26. Micali G, Aquino G, Richards DM, Endres RG (2015) Accurate encoding and decoding by single cells: amplitude versus frequency modulation. PLoS Comput Biol 11: e1004222.

27. Csanády L, Vergani P, Gadsby DC (2010) Strict coupling between CFTR's catalytic cycle and gating of its Cl^- ion pore revealed by distributions of open channel burst durations. Proc Natl Acad Sci USA 107: 1241–1246.

28. Doan T, Mendez A, Detwiler PB, Chen J, Rieke F (2006) Multiple phosphorylation sites confer reproducibility of the rod's single-photon responses. Science 313: 530–533.

29. Koshland Jr DE, Goldbeter A, Stock JB (1982) Amplification and adaptation in regulatory and sensory systems. Science 217: 220–225.

30. Ozbudak EM, Thattai M, Lim HN, Shraiman BI, van Oudenaarden A (2004) Multistability in the lactose utilization network of Escherichia coli. Nature 427: 737–740.

31. Cooper RM, Wingreen NS, Cox EC (2012) An excitable cortex and memory model successfully predicts new pseudopod dynamics. PLoS One 7: e33528.

32. Westendorf C, Negrete Jr J, Bae AJ, Sandmann R, Bodenschatz E, et al. (2013) Actin cytoskeleton of chemotactic amoebae operates close to the onset of oscillations. Proc Natl Acad Sci USA 110: 3853–3858.

33. Berezhkovskii A, Szabo A, Greives N, Zhou HX (2014) Multidimensional reaction rate theory with anisotropic diffusion. J Chem Phys 141: 204106.

34. Pollak E, Talkner P (2005) Reaction rate theory: what it was, where it is today, and where it is going. CHAOS 15: 026116.

35. Endres RG, Wingreen NS (2009) Accuracy of direct gradient sensing by cell-surface receptors. Prog Biophys Mol Biol 100: 33–39.

36. Bialek W, Setayeshgar S (2008) Cooperativity, sensitivity, and noise in biochemical signaling. Phys Rev Lett 100: 258101.

37. Berezhkovskii AM, Szabo A (2013) Effect of ligand diffusion on occupancy fluctuations of cell-surface receptors. J Chem Phys 139: 121910.

38. Kaizu K, de Rone W, Paijmans J, Takahashi K, Tostevin F, et al. (2014) The Berg-Purcell limit revisted. Biophys J 106: 976–985.

39. Agmon N, Szabo A (1990) Theory of reversible diffusion-influenced reactions. J Chem Phys 92: 5270.

40. Perkins TJ, Swain PS (2009) Strategies for cellular decision-making. Mol Syst Biol 5: 326.

41. Siggia ED, Vergassola M (2013) Decisions on the fly in cellular sensory systems. Proc Natl Acad Sci USA 110: E3704–E3712.

42. Wald A (1945) Sequential tests of statistical hypotheses. Ann Math Stat 16: 117–186.

43. Little SC, Tikhonov M, Gregor T (2013) Precise developmental gene expression arises from globally stochastic transcriptional activity. Cell 154: 789–800.

44. Tweedy L, Meier B, Stephan J, Heinrich D, Endres RG (2013) Distinct cell shapes determine accurate chemotaxis. Sci Rep 3: 2606.

45. Bicknell BA, Dayan P, Goodhill GJ (2015) The limits of chemosensation vary across dimensions. Nat Commun 6: 7468.

46. Murugan A, Huse DA, Leibler S (2012) Speed, dissipation, and error in kinetic proofreading. Proc Natl Acad Sci USA 109: 12034-12039.

47. Skoge M, Naqvi S, Meir Y, Wingreen NS (2013) Chemical sensing by nonequilibrium cooperative receptors. Phys Rev Lett 110: 248102.

48. Toyabe S, Sagawa T, Ueda M, Muneyuki E, Sano M (2010) Experimental demonstration of information-to-energy conversion and validation of the generalized Jarzynski equality. Nature Phys 6: 988–992.

49. Bérut A, Arakelyan A, Petrosyan A, Ciliberto S, Dillenschneider R, et al. (2012) Experimental verification of Landauer's principle linking information and thermodynamics. Nature 483: 187–189.

50. Barato AC, Hartich D, Seifert U (2014) Efficiency of cellular information processing. New J Phys 16: 103024.

51. Levine JH, Lin Y, Elowitz MB (2013) Functional roles of pulsing in genetic circuits. Science 6: 1193–1200.

Supplementary Information to:
Know the single-receptor sensing limit? Think again.

Gerardo Aquino[1], Ned S. Wingreen[2] and Robert G. Endres[1]

1   Berg-Purcell limit

Consider a receptor which binds and unbinds ligand molecules with kinetics for the average occupancy $\Gamma(t)$ given by

$$\frac{d\Gamma}{dt} = k_+ c_0 (1 - \Gamma) \ - \ k_- \Gamma, \tag{14}$$

where $k_+ c_0$ is the rate of binding at ligand concentration c and k_- is the rate of unbinding. At steady state, the probability of being occupied is given by $p = c_0/(c_0 + K_D)$ with the ligand dissociation constant $K_D = k_-/k_+$.

What is the uncertainty $\langle \delta c^2 \rangle$ in measuring ligand concentration c_0? If we have the uncertainty in occupancy, $\langle \delta \Gamma^2 \rangle$, we can use error propagation and write for the relative uncertainty in ligand concentration

$$\frac{\langle \delta c^2 \rangle}{c_0^2} = \left(c \frac{\partial p}{\partial c} \right)^{-2} \langle \delta \Gamma^2 \rangle \tag{15}$$

with the term in bracket evaluated at c_0.

To obtain $\langle \delta \Gamma^2 \rangle$ we could be tempted to use the variance of a Bernoulli random variable, given by $p(1-p)$. We would thus obtain $\langle \delta c^2 \rangle / c_0{}^2 = [p(1-p)]^{-1} \geq 4$ and hence at least 400% fractional error. This instantaneous error based on a single measurement in time can formally be derived as follows, which comes in handy later. Equation 14 can be linearised around the steady-state value by introducing $\Gamma(t) = p + \delta \Gamma(t)$ with $\delta \Gamma(t)$ the fluctuations and keeping only terms linear in $\delta \Gamma(t)$. This produces

$$\frac{d(\delta \Gamma)}{dt} = -(k_+ c_0 + k_-) \delta \Gamma + \eta_\Gamma \tag{16}$$

with $\eta_\Gamma(t)$ the fluctuating source, given by white noise with zero average. (That such a linearization is valid for underlying binary dynamics was shown in [1].) Subsequent Fourier transformation from the time to the frequency domain leads to

$$- i\omega \delta \hat{\Gamma} = -(k_+ c_0 + k_-) \delta \hat{\Gamma} + \hat{\eta}_\Gamma, \tag{17}$$

where we applied the Fourier transforms $\Gamma(t) = \int \frac{d\omega}{2\pi} e^{-i\omega t} \delta \hat{\Gamma}(\omega)$ and $\eta_\Gamma(t) = \int \frac{d\omega}{2\pi} e^{-i\omega t} \delta \hat{\eta}_\Gamma(\omega)$. The power spectrum is then obtained as

$$\langle \delta \hat{\Gamma}(\omega) \delta \hat{\Gamma}^*(\omega) \rangle = \langle |\delta \hat{\Gamma}^2(\omega)|^2 \rangle = \frac{Q_\Gamma}{\lambda_\Gamma^2 + \omega^2} \tag{18}$$

with noise strength $Q_\Gamma = \langle |\hat{\eta}_\Gamma(\omega)|^2 \rangle = 2 k_+ c_0 (1 - p)$ determined from Poisson statistics and frequency cut-off $\lambda_\Gamma = k_+ c_0 + k_-$. The variance is obtained by integrating the power spectrum over all frequencies

$$\langle \delta \Gamma^2 \rangle = \int \frac{d\omega}{2\pi} \langle |\delta \hat{\Gamma}(\omega)|^2 \rangle = \frac{Q_\Gamma}{2\lambda_\Gamma} = p(1-p). \tag{19}$$

In contrast, Berg and Purcell (BP) considered that the receptor has some time T available in order to produce a measurement. We expect the longer the averaging time the more accurate the measurement. Imagine a binary time series of occupancy $\Gamma(t)$ recorded for time T. The BP limit can be derived by estimating the average receptor occupancy p from the time-averaged value $\Gamma_T = 1/T \int dt\, \Gamma(t)$ with the variance given by $\langle \delta \Gamma_T^2 \rangle = \langle \Gamma_T^2 \rangle - \langle \Gamma_T \rangle^2$. The variance can be determined from the autocorrelation function of the occupancy, or equivalently the power spectrum. Specifically, the uncertainty of the occupancy $\delta \Gamma_T^2$ can be calculated by using the low-frequency limit of Eq. 18

$$\langle \delta \Gamma_T^2 \rangle = \frac{\langle |\delta \hat{\Gamma}(\omega \approx 0)|^2 \rangle}{T} = \frac{2p^2(1-p)}{k_+ c_0 T}. \tag{20}$$

When plugged into Eq. 15, this reproduces the BP limit

$$\frac{\langle \delta c^2 \rangle}{c_0^2} = \frac{2\tau_b}{Tp} = \frac{2}{\bar{N}} \tag{21}$$

with the average number of binding/unbinding events given by $\bar{N} = T/(\tau_b + \tau_u)$ with $\tau_b = k_-^{-1}$ and $\tau_u = (k_+ c_0)^{-1}$ the average bound and unbound time intervals.

2   Receptor with downstream signalling

In addition to the receptor, let us consider a signalling molecule that is produced by the ligand-bound receptor, characterised by occupancy $\Gamma(t)$. The kinetics for the copy number $n(t)$ of this signalling molecule is given by

$$\frac{dn}{dt} = k\Gamma - \tau^{-1} n, \tag{22}$$

where k times Γ is the rate of production and τ is the lifetime of the signalling molecule. At steady state, the copy number is given by $\bar{n} = k\tau p$. Using error propagation once more, we can write

$$\frac{\langle \delta c^2 \rangle}{c_0^2} = \left(c \frac{\partial \bar{n}}{\partial c} \right)^{-2} \langle \delta n^2 \rangle \tag{23}$$

with the term in parentheses evaluated at c_0. The error based on time averaging by T can be derived as before. Equation 22 can be linearised by introducing $n(t) = \bar{n} + \delta n(t)$, producing

$$\frac{d(\delta n)}{dt} = k\delta\Gamma - \tau^{-1}\delta n + \eta_n \tag{24}$$

with $\eta_n(t)$ the fluctuating source, given again by white noise with zero average. Subsequent Fourier transforming from the time to the frequency domain leads to

$$(\tau^{-1} - i\omega)\delta\hat{n} = k\delta\hat{\Gamma} + \hat{\eta}_n, \tag{25}$$

where we applied the additional Fourier transforms $n(t) = \int \frac{d\omega}{2\pi} e^{-i\omega t} \delta\hat{n}(\omega)$ and $\eta_n(t) = \int \frac{d\omega}{2\pi} e^{-i\omega t} \delta\hat{\eta}_n(\omega)$. The power spectrum is then obtained as

$$\langle |\delta\hat{n}^2(\omega)|^2 \rangle = \frac{Q_n}{\tau^{-2} + \omega^2} + \frac{Q_\Gamma k^2}{(\tau^{-2} + \omega^2)(\lambda_\Gamma^2 + \omega^2)} \tag{26}$$

with noise strength $Q_n = \langle |\hat{\eta}_n(\omega)|^2 \rangle = 2kp$ determined from Poisson statistics. The variance is obtained by calculating the time-averaged low-frequency limit

$$\langle \delta n_T^2 \rangle = \frac{\langle |\delta\hat{n}(\omega \approx 0)|^2 \rangle}{T} = 2\bar{n} \left[1 + \frac{\bar{n}(1-p)}{k_+ c_0 \tau} \right] \frac{\tau}{T}. \tag{27}$$

When plugged into Eq. 23, this produces the following limit

$$\frac{\langle \delta c^2 \rangle}{c_0^2} = \left[\frac{2}{\bar{N}_\tau} + \frac{2}{\bar{n}(1-p)^2} \right] \frac{\tau}{T} = \frac{2}{\bar{N}} + \frac{2}{\bar{n}(1-p)^2} \frac{\tau}{T} \tag{28}$$

with $\bar{N}_\tau = \tau/(\tau_b + \tau_u)$ the average number of ligand binding/unbinding events in time interval τ and $\bar{N}$ the average number in time T. The first term in Eq. 28 is the BP limit (cf. Eq. 21). The second term in Eq. 28 is due to Poisson-like number fluctuations in the signalling molecule and could be reduced for large numbers of signalling molecules. Hence the best one can do with an equilibrium receptor is the BP limit.

3   Maximum-likelihood estimation without ligand rebinding

Let N be a fixed number of subsequent bound and unbound time intervals (not the average number $\bar{N}$ here), the probability (likelihood) for such a sequence of intervals $\vec{\tau} = (\tau_1, \cdots \tau_N)$ is:

$$P(\vec{\tau}, c) \propto e^{-k_- T_b} e^{-k_+ c T_u} k_-^N (k_+ c)^N, \tag{29}$$

where $T_b = \sum_{i=1}^N \tau_b^i$ and $T_u = \sum_{i=1}^N \tau_u^i$ are the total bound and unbound times (with $T_b \simeq N\langle \tau_u \rangle$ and $T_u \simeq N\langle \tau_u \rangle$ for N large). Maximising with respect to c leads to:

$$\frac{dP}{dc} = -k_+ T_u P + \frac{N}{c} P = 0 \;\; \rightarrow \;\; c_{ML} = \frac{N}{k_+ T_u}, \tag{30}$$

i.e. c_{ML} is the concentration value that maximises the likelihood. The uncertainty in concentration measurement can be obtained from the Cramér-Rao bound which connects the uncertainty in concentration to the Fisher information.

Assume a set of measurements $\vec{\tau}$ distributed according to $P(\vec{\tau}, c)$ from which an unbiased estimation of the concentration c_0 is performed. In general it can be shown that given a set of measurements the variance for the expected value of c is bound from below by the Fisher information, i.e.

$$\langle \delta c^2 \rangle = \langle (\hat{c} - c_0)^2 \rangle \geq \frac{1}{I(c_0)}, \tag{31}$$

with $\hat{c}$ the estimated value of the true concentration c_0 and the Fisher information $I(c)$ defined as:

$$I(c) = -\int d\vec{\tau} \frac{\partial^2 \log P(\vec{\tau}, c)}{\partial c^2} P(\vec{\tau}, c) \tag{32}$$

Using Eq. (29) it follows that

$$-\frac{\partial^2 \log P(\vec{\tau}, c)}{\partial c^2} = \frac{N}{c^2}, \tag{33}$$

which, when inserted in Eq. (32), leads to $I(c) = N/c^2$. In the large-N limit the Cramér-Rao bound becomes an equality and translates into the following expression for the uncertainty in concentration sensing at c_0:

$$\frac{\langle \delta c_{ML}^2 \rangle}{c_0^2} = \frac{1}{c_0^2 I(c_0)} = \frac{1}{N}. \tag{34}$$

This result is two-fold lower than the BP limit. The difference is that the maximum-likelihood (ML) estimate considers only the unbound time intervals, as only these contain information about the ligand concentration.

A few comments are in order: The exact expectation value for the estimator can easily be derived from Eq. (30) leading to

$$\langle c_{ML} \rangle = \frac{N}{k_+} \left\langle \frac{1}{T_u} \right\rangle. \tag{35}$$

The probability density for the variable $T_u = \sum_{i=1}^N \tau_u^i$, i.e. of having a sequence of N unbound time intervals, is the N-times convolution of the single probability density $k_+ c_0 e^{-k_+ c_0 \tau_u}$, namely

$$\psi(T_u) = (k_+ c_0)^N e^{-k_+ c_0 T_u} \frac{T_u^{N-1}}{(N-1)!} \tag{36}$$

from which it follows that

$$\left\langle \frac{1}{T_u^m} \right\rangle = \int_0^\infty \frac{1}{T_u^m} \psi(T_u) dT_u = \frac{(N-1-m)!}{(N-1)!} (k_+ c_0)^m. \tag{37}$$

From Eq. (37) one can easily derive $\langle 1/T_u \rangle = \frac{k_+ c_0}{N-1}$, which, by means of Eq. (35), leads to

$$\langle c_{ML} \rangle = c_0 \frac{N}{N-1}. \tag{38}$$

It follows that the estimator is unbiased (i.e. $\langle c_{ML} \rangle = c_0$) only in the asymptotic limit of large N. The results obtained here and in the main text are consistent with this limit. From Eq. (37) evaluated for $m = 2$ one can derive as well the variance for the ML estimator

$$
\begin{aligned}
\langle \delta c_{ML}^2 \rangle &= \langle c_{ML}^2 - \langle c_{ML} \rangle^2 \rangle = \frac{N^2}{k_+^2} \left\langle \frac{1}{T_u^2} \right\rangle - \langle c_{ML} \rangle^2 = \frac{c_0^2}{N-2} \left(\frac{N}{N-1} \right)^2 \\
&\simeq_{N \gg 1} \frac{c_0^2}{N} + O(1/N^2).
\end{aligned} \tag{39}
$$

It follows that the exact value for the bound on the variance of the ML estimator is $\frac{c_0^2}{N-2} \left(\frac{N}{N-1} \right)^2$, which coincides with c_0^2/N in the $N \gg 1$ limit apart from terms of order $O(N^{-2})$. The limit of large N is consistent with the assumption that $T_u \gg k_+ c_0, k_-$ implied in the integration carried out in Eq. (37). Note that one can also define the unbiased estimator $c'_{ML} = \frac{N-1}{N} c_{ML}$ for which (using Eq. (39)) one obtains a sharper bound on the variance, given by $\langle (\delta c'_{ML})^2 \rangle = c_0^2/(N-2)$. In summary, by not using the peak value of the likelihood but the mean value, we obtain an unbiased estimator with a slightly lower uncertainty, i.e. $1/(N-2)$ instead of $1/(N-2)[N/(N-1)]^2$.

4 Bayesian Cramér-Rao bound including a prior

Next we consider cells which preserve a memory of previous environmental conditions. Specifically, the Bayesian Cramér-Rao bound [2–4] allows us to estimate a lower bound to the variance of the expected value of an estimator when a prior distribution for such an estimator is known. Let us call $\hat{c}$ the unbiased estimator of the true concentration c_0. Such a parameter is estimated based on a set of measurements $\vec{\tau}$ distributed according to $P(\vec{\tau}, c)$. If $\lambda(c)$ is the known prior distribution of the parameter c_0, then it can be shown that

$$\langle \delta c^2 \rangle = \langle (\hat{c} - c_0)^2 \rangle \geq \frac{1}{I(\lambda) + I(c_0)}, \tag{40}$$

where averaging on the left-hand side is conducted using the prior distribution, leading to the reduction in uncertainty on the right-hand side. Specifically,

$$I(\lambda) = \int dc \lambda(c) \left[\frac{\partial \log \lambda(c)}{\partial c} \right]^2 \tag{41}$$

is the contribution to the Fisher information from the prior distribution and

$$I(c) = \int dc \lambda(c) \int d\vec{\tau} P(\vec{\tau}, c) \left[\frac{\partial \log P(\vec{\tau}, c)}{\partial c} \right]^2 = -\int dc \lambda(c) \int d\vec{\tau} P(\vec{\tau}, c) \frac{\partial^2 \log P(\vec{\tau}, c)}{\partial^2 c} \tag{42}$$

is the Fisher information about the parameter c_0 given the data $\vec{\tau}$. The second equality in Eq. (42) follows from the relation $\frac{\partial^2 \log P(\vec{\tau}, c)}{\partial^2 c} = \frac{P''}{P} - \frac{P'^2}{P^2} = \frac{P''}{P} - \left[\frac{\partial \log P(\vec{\tau}, c)}{\partial c} \right]^2$ and that the term $\frac{P''}{P}$ gives zero contribution as can be checked by differentiating with respect to c the normalisation condition

$$\int d\vec{\tau} P(\vec{\tau}, c) = 1. \tag{43}$$

4.1 Log-normally distributed prior

We first consider the case where the prior distribution has a log-normal form, i.e.:

$$\lambda(c) = \frac{1}{\sigma\sqrt{2\pi}c} \exp\left[-\frac{(\log(c) - \mu)^2}{2\sigma^2}\right] \tag{44}$$

with mean and variance in log-space given by $\langle \log(c) \rangle = \mu$ and $\langle [\log(c) - \mu]^2 \rangle = \sigma$, respectively. In linear space these are given by respective expressions

$$\langle c \rangle = \exp\left(\mu + \sigma^2/2\right) \tag{45a}$$

$$\langle c^2 - \langle c \rangle^2 \rangle = \exp[2(\mu + \sigma^2)] - \exp\left(2\mu + \sigma^2\right) = \exp\left(2\mu + \sigma^2\right)\left[\exp\left(\sigma^2\right) - 1\right]. \tag{45b}$$

Consequently, $I(\lambda)$ is given by:

$$\begin{aligned}
I(\lambda) &= \int dc \lambda(c) \left[\frac{\partial \log \lambda(c)}{\partial c}\right]^2 = \int \frac{dc}{c_0^2}\left[\frac{1}{\sigma^2}(\log(c) - \mu) + 1\right]^2 \exp\left[-\frac{(\log(c) - \mu)^2}{2\sigma^2}\right] \\
&= \left(\frac{1}{\sigma^2} + 1\right) \exp\left[-2(\mu - \sigma^2)\right]
\end{aligned} \tag{46}$$

Furthermore, $I(c)$ follows from Eq. (32) where $P(\vec{\tau}, c)$, the probability (likelihood) of observing a sequence $\vec{\tau}$ of N bound and unbound time intervals, is given by Eq. (29). Equations (29) and (30) lead to the following expression for $I(c)$:

$$I(c) = \int dc \int d\vec{\tau} P(\vec{\tau}, c)\frac{N}{c^2}\lambda(c). \tag{47}$$

Performing the integration in $\vec{\tau}$ due to the normalisation condition, we obtain:

$$I(c) = \int dc \frac{N}{c^2}\lambda(c) = N \exp[-2(\mu - \sigma^2)]. \tag{48}$$

In conclusion, the uncertainty in ligand concentration with the Bayesian Cramér-Rao bound and a log-normal prior is given by

$$\langle \delta c^2 \rangle \geq \frac{\exp[2(\mu - \sigma^2)]}{N + 1/\sigma^2 + 1}. \tag{49}$$

In the following we deviate slightly from the derivation found in [5]. In this article the prior was assumed to be centred around the true ligand concentration. Here, we assume more conservatively that the prior distribution is centred around the (erroneous) ML value c_{ML} of the concentration obtained from the previous measurement. The variance of the distribution is again given by the standard Cramér-Rao bound from the ML estimation, $\langle \delta c_{ML}^2 \rangle = c_0^2/N$ [6] with c_0 the true value for the concentration. From these assumptions it follows that

$$\langle c \rangle = \exp\left[\mu + \frac{\sigma^2}{2}\right] = c_{ML} \tag{50a}$$

$$\langle c^2 - \langle c \rangle^2 \rangle = \left(\exp(\sigma^2) - 1\right) \langle c \rangle^2 = \frac{c_0^2}{N}, \tag{50b}$$

where last equality follows from Eq. (34). We can now express σ^2 in terms of known quantities, noticing that, for large number of events N, from Eq. (50b) it follows:

$$\exp[\sigma^2] - 1 \simeq \frac{1}{N} \quad \rightarrow \quad \sigma^2 \simeq \log\left(1 + \frac{1}{N}\right) \simeq \frac{1}{N}. \tag{51}$$

Inserting this expression for σ^2 into Eq. (49) leads to $\langle \delta c^2 \rangle \geq \frac{c_{ML}^2 e^{-3/N}}{N+1/N+1}$ and therefore to

$$\frac{\langle \delta c^2 \rangle}{c_0^2} \geq \frac{1}{2N}, \tag{52}$$

where c_0 in the denominator is the true value of the concentration, which differs from c_{ML} obtained from previous measurement by at most a correction proportional to $c_0/\sqrt{N}$ (due to Eq. (34)), so that Eq. (52) is correct to leading order for N large, a result identical to the one in [5].

Eq. (52) means that having a prior distribution for N intervals is the same as measuring for $2N$ intervals without a prior distribution. Hence, information is neither lost nor gained. This also means that by using memory (in the form of a prior) a cell can effectively perform longer and hence more accurate measurements without being limited by the actual measurement (averaging) time.

4.2 Gamma-distributed prior

Alternatively, assume the prior is given by the Gamma distribution

$$\lambda(c) = \frac{c^{\alpha-1}\gamma^\alpha e^{-\gamma c}}{\Gamma[\alpha]}, \tag{53}$$

where the parameters α and γ are related to the first and second moment of the distribution:

$$\langle c \rangle = \frac{\alpha}{\gamma} \tag{54a}$$

$$\langle c^2 - \langle c \rangle)^2 \rangle = \frac{\alpha}{\gamma^2}. \tag{54b}$$

For such a prior distribution, $I(\lambda)$ reads:

$$I(\lambda) = \int \left[\frac{\partial \log \lambda(c)}{\partial c} \right]^2 \lambda(c) dc = \tag{55}$$
$$\int \frac{\lambda'(c)^2}{\lambda(c)} dc = \int_0^\infty dc \frac{e^{-\gamma c}(\gamma c)^{\alpha+1}(\alpha-1-\gamma c)^2}{\gamma c^4 \Gamma[\alpha]} = \frac{\gamma^2}{\alpha-2}.$$

The Fisher information $I(c)$ is determined from Eq. (47) using the Gamma distribution instead of the log-normal distribution

$$I(c) = \int dc \int d\vec{\tau} P(\vec{\tau}, c) \frac{N}{c^2} \lambda(c) = \tag{56}$$
$$\int \frac{N}{c^2} \lambda(c) dc = N\gamma^2 \int_0^\infty dc \frac{c^{\alpha-3} e^{-\gamma c} \gamma^{\alpha-2}}{\Gamma[\alpha]} = \frac{N\gamma^2}{(\alpha-1)(\alpha-2)}.$$

Consequently, the Bayesian Cramér-Rao bound is given by:

$$\langle \delta c^2 \rangle \geq \frac{1}{\frac{\gamma^2}{\alpha-2} + \frac{N\gamma^2}{(\alpha-1)(\alpha-2)}}. \tag{57}$$

With the same assumptions as done in the previous section, mean value and standard deviation of the prior distribution are set to c_{ML} and c_{ML}^2/N, respectively (see Eqs. (50)), with c_{ML} the ML value for the concentration obtained in previous measurement. Eqs. (54a) and (54b) then imply:

$$\gamma = \frac{N}{c_{ML}} \tag{58a}$$

$$\alpha = N. \tag{58b}$$

In the limit of large N, this leads to relative uncertainty

$$\frac{\langle \delta c^2 \rangle}{c_0^2} \geq \frac{1}{\frac{N^2}{(N-2)} + \frac{N^3}{(N-1)(N-2)}} \simeq \frac{1}{2N}, \tag{59}$$

with again c_0 the true value of the concentration ($c_{ML} \simeq c_0 \pm c_0/\sqrt{N}$). Not surprisingly, this is the same result as obtained in Eq. (52), since both the log-normal and the Gamma distribution can be derived from Gaussian distributed variables. The Gamma distribution is the distribution of the sum of squared normal variables (a.k.a. χ^2 distribution), while the log-normal, as the name suggests, is the distribution of the logarithm of a normally distributed variable.

5 Maximum-likelihood estimation with ligand rebinding

Endres and Wingreen [6] applied maximum likelihood (ML) to the problem of estimating the ligand concentration from a time series of ligand-receptor occupancy, but focused on the uncertainty of this measurement without ligand rebinding, i.e. effectively for very fast diffusion. For slower diffusion one should consider possible rebinding of a previously bound ligand molecule, which makes the instantaneous rate of binding a functional of the previous binding and unbinding events. The binding rate can thus be written as $k_+ c_0(t, \{t_+, t_-\})$. The rate of unbinding remains k_-, so the ML estimate of concentration still comes entirely from the durations of the unbound intervals.

We quickly review ML estimation of the ligand concentration with ligand rebinding [6]. The probability for a time series to occur given a ligand concentration c_0 is

$$P(\{t_+, t_-\}; c) = \prod_i p_b(t_{+,i}, t_{-,i}) p_-(t_{-,i}) p_u(t_{-,i}, t_{+,i+1}) p_+(t_{+,i+1}), \tag{60}$$

where the probability for a ligand molecule to remain bound from $t_{+,i}$ to $t_{-,i}$ is

$$p_b(t_{+,i}, t_{-,i}) = p_b(t_{-,i} - t_{+,i}) = e^{-k_-(t_{-,i} - t_{+,i})}. \tag{61}$$

The probability for a receptor to remain unbound from $t_{-,i}$ to $t_{+,i+1}$ includes the effect on the binding of the changing concentration of ligand $p_+ \propto k_+(c_0 + \Delta c_i)$ where Δc_i is the perturbation to the ligand concentration from previous binding and unbinding events. Consequently

$$p_u(t_{-,i}, t_{+,i+1}) = e^{-k_+ c_0(t_{+,i+1} - t_{-,i}) - k_+ \int_i \Delta c(t') dt'}, \tag{62}$$

where we have expressed the ligand concentration as

$$c(t, \{t_+, t_-\}) = c_0 + \Delta c(t, \{t_+, t_-\}) = c_0 + \Delta c(\{t - t_{-,i}; t - t_{+,i}\}), \tag{63}$$

and used the notation $\int_i dt' = \int_{t_{-,i}}^{t_{+,i+1}} dt'$, $\Delta c(t') = \Delta c(t', \{t_+, t_-\})$, and $\Delta c_i = \Delta c(t_{+,i})$.

The terms can be gathered as before, leading to

$$P(\{t_+, t_-\}; c) \propto e^{-k_- T_b} \cdot e^{-k_+ c_0 T_u} \cdot k_-^N \cdot k_+^N \cdot \prod_i (c_0 + \Delta c_i) e^{-k_+ \int_i \Delta c(t') dt'}. \tag{64}$$

Importantly, all the Δc's depend only on the times of events, not the value of c_0, so $d(\Delta c)/dc = 0$, yielding

$$\frac{dP}{dc} \propto -k_+ T_u P + \sum_i \frac{1}{c_0 + \Delta c_i} P. \tag{65}$$

Setting the above derivative to zero yields an implicit equation for the ML estimate of c_0,

$$\sum_i \frac{1}{c_0 + \Delta c_i} = k_+ T_u, \tag{66}$$

where the sum is over all binding events. Importantly, each Δc_i depends deterministically on all previous binding and unbinding events. For the special case of fast diffusion $D = \infty$ and hence $\Delta c_i = 0$, we obtain [6] $k_+ c_0 = N/T_u = 1/\langle \tau_u \rangle$ where T_u is the total unbound time of the receptor during time T, N is the total number of binding/unbinding events, and $\langle \tau_u \rangle$ is the average unbound time interval.

How accurate is the concentration estimate? Using the Cramér-Rao bound once more, we obtain for the normalised variance

$$\frac{\langle \delta c^2 \rangle}{c_0^2} = -\frac{1}{c_0^2 \left\langle \frac{d^2 \ln(P)}{dc^2} \right\rangle_{c_0}} = \frac{1}{\langle \sum_i (1 + \Delta c_i/c_0)^{-2} \rangle_{c_0}}, \tag{67}$$

where we used P from Eq. 64. Hence, the normalised variance of the ML estimate of the true concentration c_0 is the inverse of the number of unbound intervals with additional corrections in the regime of slow diffusion, due to perturbations in ligand concentration from previous binding and unbinding events.

Equation 67 depends on the average over all trajectories with N binding and unbinding events. Furthermore, each perturbation in ligand concentration, Δc_i, depends on the whole history of binding and unbinding events, making this equation unsolvable. However, we can estimate the effect of diffusion in the limit of slow binding and unbinding, or fast diffusion. Hence, for small $\Delta c_i/c$, we can expand to linear order

$$\frac{\langle \delta c^2 \rangle}{c_0^2} \approx \frac{1}{N} \left(1 + 2 \frac{\langle \Delta c \rangle}{c_0} \right) \tag{68}$$

to simplify the equation for the uncertainty. Equation 68 now contains only a typical perturbation in ligand concentration $\langle \Delta c \rangle$. To estimate this we use the solution of the diffusion equation for a single ligand molecule

$$\Delta_\pm c(\vec{r}, t) = \frac{\pm 1}{(4\pi D t)^{d/2}} e^{-\frac{r^2}{4Dt}}, \tag{69}$$

with $+1$ corresponding to an unbound ligand molecule (source) and -1 corresponding to a bound ligand molecule (sink) at $t = 0$. We assume the receptor sits at $\vec{r} = 0$, at which we wish to evaluate perturbation. Here, we provide results for dimensions $d = 2$ and 3.

2-dimensional diffusion: Here we consider $d = 2$ in Eq. 69. To further simplify the calculation of the whole history of binding and unbinding events, we assume all binding events are independent, i.e. only depend on the average rate $k_+ c_0$ and not also on the perturbations. We thus obtain the infinite series

$$\langle \Delta c(t) \rangle = \frac{1}{4\pi D} \left(\left\langle \frac{1}{\tau_1} \right\rangle - \left\langle \frac{1}{\tau_1 + \tau_2} \right\rangle + ... (-1)^{K+1} \left\langle \frac{1}{\tau_1 + \tau_2 + ... + \tau_K} \right\rangle + ... \right), \tag{70}$$

with the most recent (unbinding) event occurring at time $t - \tau_1$ and increasing the overall concentration (source) and the second most recent (binding) event occurring at time $t - (\tau_1 + \tau_2)$ and decreasing the overall concentration (sink), and so on. The averages are performed over the probability of a sequence of K events and then summed in the limit $K \to \infty$ to account for an infinitely long history.

For the special case $p = 1/2$, so that $\langle \tau_u \rangle = \langle \tau_b \rangle = \tau$ and $\lambda = k_+ c_0 = k_-$, each random number τ is generated with the same distribution $\psi(\tau) = \lambda e^{-\lambda \tau}$. In order to evaluate the generic term in the series of Eq. (70) one has first to evaluate the probability density that a given value T_K is obtained for the

sum $\sum_{i=1}^{K} \tau_i = T_K$ after K draws of the random variable τ. This probability is given by the K-times convolution of the distribution $\psi(\tau)$, which is:

$$\psi_K(T_K) = \lambda^K e^{-\lambda T_K} \frac{T_K^{K-1}}{(K-1)!}. \tag{71}$$

Then, by using this distribution one can evaluate $\langle \frac{1}{T_K} \rangle$. This allows us to obtain an expression for a generic term with $K \geq 2$ in the sum in Eq. (70), leading to

$$\left\langle \frac{1}{T_K} \right\rangle = \int_0^\infty \frac{1}{T_K} \psi_K(T_K) dT_K = \frac{\lambda}{K-1}. \tag{72}$$

Summing all these contributions for $K \geq 2$ leads to

$$\sum_{K=2}^\infty (-1)^{K+1} \frac{\lambda}{K-1} = -\lambda \log 2. \tag{73}$$

The contribution for $K = 1$ has to be calculated separately. In fact, one has to calculate $\langle 1/\tau \rangle = \lambda \int_0^\infty dt\, e^{-\lambda t}/t$, which is the Gamma function $\Gamma(n)$ for diverging parameter $n = -1$. To make progress we realise that the maximal perturbation is the change in concentration due to a single ligand molecule released into a $2D$ area of the order of the size of the binding site, so $\Delta c_{+,max} \simeq 1/a^2 = \frac{1}{4\pi D \tau_a}$. This effectively introduces a minimal time $\tau_a = a^2/(4\pi D)$. As a result, we approximate the integral by

$$\left\langle \frac{1}{\tau} \right\rangle = \lambda \int_{\tau_a}^\infty dt \frac{e^{-\lambda t}}{t} = -\lambda \text{Ei}(-x) = -\lambda \left[\gamma + \ln x + \sum_{k=1}^\infty (-1)^k \frac{x^k}{k(k!)} \right] \tag{74}$$

with $x = k_+ c_0 \tau_a \ll 1$ and hence $\ln x \ll 0$, and $\gamma \approx 0.57721...$ the Euler-Mascheroni constant. For very small x, γ and the sum can be neglected and the dominant term is the logarithmic part. In this limit it is evident as well that the contribution of the most recent event is much larger than the contribution from all other events in Eq. (73), so that the final result is

$$\langle \Delta c \rangle \approx \frac{k_+ c_0}{4\pi D} \ln \left(\frac{4\pi D}{k_+ c_0 a^2} \right), \tag{75}$$

showing the competition between rebinding with rate $k_+ c_0$ and diffusion to remove the unbound ligand molecule. As expected for 2D, this result only shows a weak dependence on diffusion and receptor size.

3-dimensional diffusion: Here we set $d = 3$ in Eq. 69 and obtain

$$\langle \Delta c \rangle = \frac{1}{(4\pi D)^{3/2}} \left(\langle \tau_1^{-3/2} \rangle - \langle (\tau_1 + \tau_2)^{-3/2} \rangle + ... (-1)^{K+1} \langle (\tau_1 + \tau_2 + ... + \tau_K)^{-3/2} \rangle ... \right). \tag{76}$$

The calculation therefore, under the simplifying assumption $\lambda = k_+ c_0 = k_-$, is analogous to the 2-dimensional case with the only difference that the average $\langle \tau^{-3/2} \rangle = \lambda \int_0^\infty d\tau e^{-\lambda \tau}/\tau^{3/2}$ replaces $\langle \tau^{-1} \rangle$. Also in this case it can be shown that the contribution from the most recent event is dominant as compared to that of all other events (i.e. terms in Eq. (76) with $K \geq 2$). Using the distribution in Eq. (71) it is possible to calculate the contributions from all the terms with $K \geq 2$ in Eq. (76). One obtains for a generic term in the sum:

$$\left\langle \frac{1}{T_K^{3/2}} \right\rangle = \int_0^\infty T_K^{-3/2} \psi_K(T_K) dT_K = \lambda^{3/2} \frac{\Gamma[K - 3/2]}{\Gamma[K]}, \tag{77}$$

which, after summation, leads to:

$$\sum_{K=2}^{\infty}(-1)^{K+1}\left\langle\frac{1}{T_K^{3/2}}\right\rangle = -2(\sqrt{2}-1)\sqrt{\pi}\lambda^{3/2}. \tag{78}$$

The contribution from the most recent event (i.e. first term in Eq. (76)) is given by $\langle\tau^{-3/2}\rangle = \lambda\int_0^{\infty}d\tau e^{-\lambda\tau}/\tau^{3/2}$. Introducing $x = k_+c_0\tau_a = \lambda\tau_a \ll 1$ as in the 2D case, the evaluation of $\langle\tau^{-3/2}\rangle$ leads to

$$\langle\tau^{-3/2}\rangle = \lambda\int_{\tau_a}^{\infty}d\tau e^{-\lambda\tau}/\tau^{3/2} = 2\lambda^{3/2}\left[\frac{e^{-x}}{\sqrt{x}} - \sqrt{\pi}\mathrm{Erf}\left(\sqrt{x}\right)\right], \tag{79}$$

which, to leading order in $x \ll 1$, leads to

$$\langle\tau^{-3/2}\rangle \simeq \frac{2\lambda}{\sqrt{a^2/(4\pi D)}}. \tag{80}$$

The ratio between the contribution from terms with $K \geq 2$ of Eq. (78) and this contribution amounts to $\sim \sqrt{\lambda\tau_a} = \sqrt{x} \ll 1$, which justifies keeping only the first term in Eq. (76) in the limit $x \ll 1$. The final result is therefore

$$\langle\Delta c\rangle \simeq \frac{1}{(4\pi D)^{3/2}}\langle\tau^{-3/2}\rangle \simeq \frac{1}{(4\pi D)^{3/2}}\frac{2k_+c_0}{\sqrt{a^2/(4\pi D)}} = \frac{k_+c_0}{2\pi Da}, \tag{81}$$

which has a stronger dependence on diffusion and receptor size compared to sensing in 2D. The results for diffusion in 2D and 3D are stated in the main text. Specifically, Eq. 12 in the main text is obtained by using $N = T_u/\langle\tau_u\rangle$ for the number of binding/unbinding intervals with $T_u = (1 - p)T$ and $\langle\tau_u\rangle = (k_+c_0)^{-1}$. Note that while we estimate $\langle\Delta c\rangle$ from the whole history of binding events, in our calculation the individual binding events depend only on the average ligand concentration c_0. Hence, similar to other derivations of the uncertainty of sensing by a receptor with ligand rebinding (main text Eqs. (10) [7] and (11) [8]), we calculate the first-order correction to the uncertainty due to ligand diffusion and rebinding. Note also that only the last unbinding event counts for deriving $\langle\Delta c\rangle$ so the exact durations of former unbound intervals do not matter.

6 Uncertainty and decision-making algorithms

Rapid and accurate decisions are ubiquitously made in cells motivating modelling of how this timely accuracy is achieved. Here, we follow Siggia and Vergassola to evaluate the decision time and uncertainty associated with optimal decision-making algorithms [9]. In particular, we want to make a connection between decision-making algorithms and ML estimation/BP limit.

In the case of deciding between two options, e.g. two concentration values c_1 and c_2, it can be shown that the Wald algorithm is, on average, optimal in time. Given a fixed probability that the wrong decision is made, the Wald algorithm makes the decision in the shortest amount of time on average. In this algorithm two fixed thresholds H_1 and $H_2 > H_1$ are given, and at each time step the ratio

$$R = L(\text{data}|c_1)/L(\text{data}|c_2) \tag{82}$$

between the likelihoods conditioned to either option is evaluated. Concentration $c_1(c_2)$ is chosen if $R \leq H_1(R \geq H_2)$, while data acquisition continues if $H_1 < R < H_2$. The algorithm can be mapped to a diffusion process of the variable $\ln R$ between two absorbing boundaries, corresponding to the thresholds, the values of which are in turn directly connected to the decision-error probability that $c_1(c_2)$ is wrongly chosen when real value is $c_2(c_1)$. In the diffusive approximation for $\ln R$ the average absorption time $\langle T_{\text{abs}}\rangle$, which coincides with the decision time, is given by [9]

$$\langle T_{\text{abs}}\rangle = \frac{x}{V} + \frac{K}{V\sinh(VK/D)}\left[\cosh(KV/D) - e^{-xV/D}\right] \tag{83}$$

with x the initial value, V the drift and D the diffusivity of $\ln R$, and symmetric absorbing boundaries at $x = \pm K = \pm\frac{1}{2}\log(\frac{H_2}{H_1})$.

7 Neyman-Pearson lemma

In the Wald algorithm time is not constrained to be fixed, and this algorithm is optimal in time on average. If time is constrained, i.e. fixed sample or data size, the optimal test is given by the Neyman-Pearson (NP) lemma. When choosing between two options c_1 (reference hypothesis) and c_2 with a criterion A for rejecting c_1 and a given probability of a decision error

$$\alpha = P(A|c_1), \tag{84}$$

i.e. of wrongly choosing c_2 when the data are generated with c_1, the optimal choice is made by rejecting c_1 in favour of c_2 if $R \leq H$ and choosing c_1 otherwise. Again, R is the likelihood ratio of Eq. (82) and H is an α-dependent threshold (NP lemma). This optimal criterion fulfils by definition the constraint of Eq. (84)

$$\alpha = P(R \leq H|c_1) = \int_{x:R\leq H} L(x|c_1)dx, \tag{85}$$

which shows also that the threshold value H is determined by α. This algorithm is optimal in the sense that any other algorithm based on a different rejection criterion A of the reference hypothesis c_1 but with the same α, will have a smaller probability $P(A|c_2)$ of correctly choosing c_2 (i.e. correctly rejecting c_1) as compared to the analogous NP's probability $P(R \leq H|c_2)$:

$$P(R \leq H|c_2) = \int_{x:R\leq H} L(x|c_2)dx \geq P(A|c_2) = \int_{x:A} L(x|c_2)dx \quad \forall A \text{ on } x. \tag{86}$$

In other words for all possible data generated with c_2 the NP test will correctly choose c_2 more often than any other test with the same α. For this reason this algorithm may be seen as a maximal-likelihood decision-making algorithm as the likelihood of correctly choosing c_2 is maximal. So while the Wald algorithm is optimal in time on average, for a fixed time the NP algorithm leads to a maximum likelihood of the correct decision.

8 Decision-making algorithms vs. Berg-Purcell limit

Berg and Purcell (BP) were the first to derive an estimate for the uncertainty of a measurement of ligand concentration in a fixed time T by a small detecting device, e.g. a cell. Here we consider their model as applied to a single receptor. As discussed, their estimate was later improved by the maximum-likelihood (ML) estimate, showing that the uncertainty is actually smaller by a factor two because only unbound intervals carry information about the external concentration [6]. Estimates for the uncertainty refer to concentration measurements and cannot directly be compared to decision making between two values.

However, one can still assume that in the BP and ML estimates, different concentrations c_1 and c_2 can be told apart if $\sqrt{\langle \delta c^2 \rangle} < |c_2 - c_1|$ and that, assuming either c_1 or c_2 as the true value, a decision error occurs if a measurement returns a value outside one standard deviation from the true value. With these choices for the thresholds one accounts for large fluctuations around the true value, which may lead to wrongly deciding on the other of two possible options for the true value. We are now in a position in which we can attempt to compare BP and ML estimates with the Wald and NP algorithms. Setting the decision error α of the Wald and NP algorithms equal to the decision error from both the BP and ML estimates introduced above, one obtains minimum value $|c_2 - c_1|$ for fixed value c_1 so that a decision

between c_2 and c_1 can be made with error α. This value can in turn be used as a definition of the uncertainty in decision making and compared to the BP and ML estimates.

Specifically, for a given value of T for the Wald algorithm one can use Eq. (83) and, for given c_1, derive the corresponding value of c_2 that can be distinguished in time T with decision error $\alpha = \alpha(K)$, with $x = \pm K$ the absorbing boundaries for the symmetric case. Using this approach, we can plot $(c_2 - c_1)^2$ of the Wald algorithm as a function of T and hence indirectly compare to the uncertainties from BP and ML (Fig. 5). A similar procedure allows us to extract $(c_2 - c_1)^2$ for the fixed-time Neyman-Pearson lemma (which is also shown in Fig. 5).

References

1. D. Clausznitzer and R.G. Endres, BMC Syst. Biol. **5**, 151 (2011).

2. H.L. Van Trees *Detection, Estimation and Modulation Theory* Part I, New York: Wiley (1968).

3. B.Z. Bobrovsky, E. Mayer-Wolf and M. Zakai, Ann. Stats. **14**: 1421-38 (1987).

4. R.D. Gill and B.Y. Levit, Bernoulli **1**: 59-79 (1995).

5. G. Aquino, L. Tweedy, D. Heinrich, R.G. Endres, Sci. Rep. **4**: 5688 (2014).

6. R.G. Endres and N. Wingreen, Phys. Rev. Lett. **103**, 158101 (2009).

7. W. Bialek and S. Setayeshgar, Proc. Natl. Acad. Sci. USA **102**, 10040 (2005).

8. K. Kaizu, W. de Ronde, J. Paijmans, K. Takahashi, F. Tostevin, P.R. ten Wolde, Biophys. J. **106**: 976 (2014).

9. E.D. Siggia and M. Vergassola, Proc. Natl. Acad. Sci. USA **110**, E3704 (2013).